Terahertz pulsed spectroscopy of freshly excised human breast cancer

Philip C. Ashworth[1,2,*], Emma Pickwell-MacPherson[3], Elena Provenzano[4], Sarah E. Pinder[5], Anand D. Purushotham[5], Michael Pepper[1,2] and Vincent P. Wallace[6,*]

[1]*Semiconductor Physics Group, Cavendish Laboratory, University of Cambridge, JJ Thompson Ave., Cambridge, CB3 0HE, UK*
[2]*TeraView Ltd., Platinum Building, St. John's Innovation Park, CB4 0WS, UK*
[3]*Department of Electronic Engineering, Chinese University of Hong Kong, HKSAR, China*
[4]*Department of Histopathology, Addenbrooke's NHS Foundation Trust, Hills Road, Cambridge, CB2 2QQ, UK*
[5]*Department of Academic Oncology, King's College London, Guy's Hospital, St. Thomas Street, London, UK*
[6]*Optical + Biomedical Engineering Laboratory, School of Electrical, Electronic and Computer Engineering, University of Western Australia, Crawley, 6009, Australia*
**pca27@cam.ac.uk, vincent.wallace@physics.org*

Abstract: The complex refractive indices of freshly excised healthy breast tissue and breast cancers collected from 20 patients were measured in the range of 0.15 – 2.0 THz using a portable terahertz pulsed transmission spectrometer. Histology was performed to classify the tissue samples as healthy adipose tissue, healthy fibrous breast tissue, or breast cancers. The average complex refractive index was determined for each group and it was found that samples containing cancer had a higher refractive index and absorption coefficient. The terahertz properties of the tissues were also used to simulate the impulse response functions expected when imaging breast tissue in a reflection geometry as in terahertz pulsed imaging (TPI). Our results indicate that both TPS and TPI can be used to distinguish between healthy adipose breast tissue, healthy fibrous breast tissue and breast cancer due to the differences in the fundamental optical properties.

OCIS codes: (000.1430) Biology and medicine; (300.6495) Spectroscopy, terahertz; (170.6510) Spectroscopy, tissue diagnostics; (170.6935) Tissue characterization.

References and links

1. P. Y. Han, G. C. Cho, and X. C. Zhang, "Time-domain transillumination of biological tissues with terahertz pulses," Opt. Lett. **25**(4), 242–244 (2000).
2. P. Haring Bolívar, M. Nagel, F. Richter, M. Brucherseifer, H. Kurz, A. Bosserhoff, and R. Büttner, "Label-free THz sensing of genetic sequences: towards 'THz biochips," Philosophical Transactions of the Royal Society of London Series A-Mathematical Physical and Engineering Sciences **362**(1815), 323–335 (2004).
3. A. G. Markelz, "Terahertz dielectric sensitivity to biomolecular structure and function," IEEE J. Sel. Top. Quantum Electron. **14**(1), 180–190 (2008).
4. B. M. Fischer, M. Walther, and P. U. Jepsen, "Far-infrared vibrational modes of DNA components studied by terahertz time-domain spectroscopy," Phys. Med. Biol. **47**(21), 3807–3814 (2002).
5. R. M. Woodward, V. P. Wallace, R. J. Pye, B. E. Cole, D. D. Arnone, E. H. Linfield, and M. Pepper, "Terahertz pulse imaging of *ex vivo* basal cell carcinoma," J. Invest. Dermatol. **120**(1), 72–78 (2003).
6. A. J. Fitzgerald, V. P. Wallace, M. Jimenez-Linan, L. Bobrow, R. J. Pye, A. D. Purushotham, and D. D. Arnone, "Terahertz pulsed imaging of human breast tumors," Radiology **239**(2), 533–540 (2006).
7. E. Pickwell, A. J. Fitzgerald, B. E. Cole, P. F. Taday, R. J. Pye, T. Ha, M. Pepper, and V. P. Wallace, "Simulating the response of terahertz radiation to basal cell carcinoma using *ex vivo* spectroscopy measurements," J. Biomed. Opt. **10**(6), 064021–064027 (2005).
8. M. Nagel, M. Forst, and H. Kurz, "THz biosensing devices: fundamentals and technology," J. Phys. Condens. Matter **18**(18), S601–S618 (2006).
9. J. R. Knab, J. Y. Chen, Y. F. He, and A. G. Markelz, "Terahertz measurements of protein relaxational dynamics," Proc. IEEE **95**(8), 1605–1610 (2007).
10. E. Berry, G. C. Walker, A. J. Fitzgerald, N. N. Zinov'ev, M. Chamberlain, S. W. Smye, R. E. Miles, and M. A. Smith, "Do in vivo terahertz imaging systems comply with safety guidelines?" J. Laser Appl. **15**(3), 192–198 (2003).
11. C. Rønne and S. R. Keiding, "Low frequency spectroscopy of liquid water using THz-time domain spectroscopy," Journal of Molecular Liquids **101**, PII S0167–7322(0102) 00093–00094 (2002).

#110869 - $15.00 USD Received 4 May 2009; revised 29 Jun 2009; accepted 29 Jun 2009; published 7 Jul 2009

12. V. P. Wallace, A. J. Fitzgerald, E. Pickwell, R. J. Pye, P. F. Taday, N. Flanagan, and T. Ha, "Terahertz pulsed spectroscopy of human Basal cell carcinoma," Appl. Spectrosc. **60**(10), 1127–1133 (2006).
13. A. Jemal, R. Siegel, E. Ward, Y. P. Hao, J. Q. Xu, and M. J. Thun, "Cancer statistics, 2009," CA Cancer J. Clin. **59**, 1–25 (2009).
14. J. R. Harris, M. E. Lippman, M. Morrow, and K. Osbourne, *Diseases of the Breast* (Lippincott, Williams & Wilkins, Philadelphia, 2004), pp. 719–744.
15. H. Madjar, H. A. Ladner, W. Sauerbrei, A. Oberstein, H. Prömpeler, and A. Pfleiderer, "Preoperative staging of breast cancer by palpation, mammography and high-resolution ultrasound," Ultrasound Obstet. Gynecol. **3**(3), 185–190 (1993).
16. P. Taday, and D. A. Newnham, "Advances in terahertz pulsed systems brings far-infrared spectroscopy into the spotlight," Spectroscopy Europe **16**, 20–24 (2004).
17. R. M. Woodward, B. E. Cole, V. P. Wallace, R. J. Pye, D. D. Arnone, E. H. Linfield, and M. Pepper, "Terahertz pulse imaging in reflection geometry of human skin cancer and skin tissue," Phys. Med. Biol. **47**(21), 3853–3863 (2002).
18. E. Berry, J. W. Handley, A. J. Fitzgerald, W. J. Merchant, R. D. Boyle, N. N. Zinov'ev, R. E. Miles, J. M. Chamberlain, and M. A. Smith, "Multispectral classification techniques for terahertz pulsed imaging: an example in histopathology," Med. Eng. Phys. **26**(5), 423–430 (2004).
19. S. Nakajima, H. Hoshina, M. Yamashita, C. Otani, and N. Miyoshi, "Terahertz imaging diagnostics of cancer tissues with a chemometrics technique," Appl. Phys. Lett. **90**(4), 041102 (2007).
20. C. Reid, A. P. Gibson, J. C. Hebden, and V. P. Wallace, "The use of tissue mimicking phantoms in analysing contrast in THz pulsed imaging of biological tissue," in *Conference Digest of the Joint 32nd International Conference on Infrared and Millimetre Waves, and 15th International Conference on Terahertz Electronics*, P. C. H. M.J.Griffin, T.J.Parker, K.P.Wood, ed. (IEEE, Cardiff, UK, 2007), pp. 567–568.
21. P. Ashworth, P. O'Kelly, A. Purushotham, S. Pinder, M. Kontos, M. Pepper, and V. Wallace, An Intra-operative THz Probe For Use During The Surgical Removal of Breast Tumors," in *33rd International Conference on Infrared, Millimeter, and Terahertz Waves*, M. P. Siegel, ed. (IEEE, Pasadena, California, 2008).

1. Introduction

In recent years there has been growing interest in the application of terahertz (THz) technology to the field of bio-medical imaging [1–6]. THz Pulsed Imaging (TPI) provides broadband (0.1 – 4 THz) information on samples making it possible to distinguish between regions with different optical characteristics over the THz frequency range. THz transmission spectroscopy or THz pulsed spectroscopy (TPS) has previously been used to obtain the THz optical characteristics of skin tissue [7], including the refractive index and absorption coefficient spectra. TPS has also been used to successfully characterize DNA [8] and proteins [9] in this range, allowing us to probe intermolecular interactions. THz wavelengths corresponding to the range previously mentioned are 3 mm to 80 μm; this is longer than that of optical or infrared, so THz radiation is less susceptible to scattering within freshly excised biological tissue [1] and in this paper we have assumed to be negligible. THz radiation has a shorter wavelength than that of microwave frequencies providing it with higher spatial resolution capabilities. The radiation is non-ionizing and power levels found in pulsed systems (<1 μW) are orders of magnitude lower than the maximum permissible beam power as determined by safety guidelines [10]. Furthermore, owing to the coherent time gated detection technique there is efficient elimination of background noise which leads to a very high signal to noise ratio (>10,000:1 at 1 THz). Terahertz radiation is uniquely sensitive to water [11] which, together with the advantages listed above, makes it a viable tool for medical imaging and in particular cancers. Previous *ex vivo* studies have shown that TPI can be used to identify basal cell carcinomas (BCC) of human skin [5,12] and in 2006 Fitzgerald *et al.* [6] showed that TPI could be used to identify contrast between healthy breast tissue and breast cancer. Figure 1 shows THz images obtained from freshly excised breast tissue [6]. By comparing parameters derived from the different shape of pulses reflected from the tissues such as the maximum or minimum electric field values of the pulse (E_{max}, E_{min}). It is suggested that this technique of imaging could be used to assist surgeons performing breast conserving surgery when excising cancers by better defining the cancer margins.

#110869 - $15.00 USD Received 4 May 2009; revised 29 Jun 2009; accepted 29 Jun 2009; published 7 Jul 2009

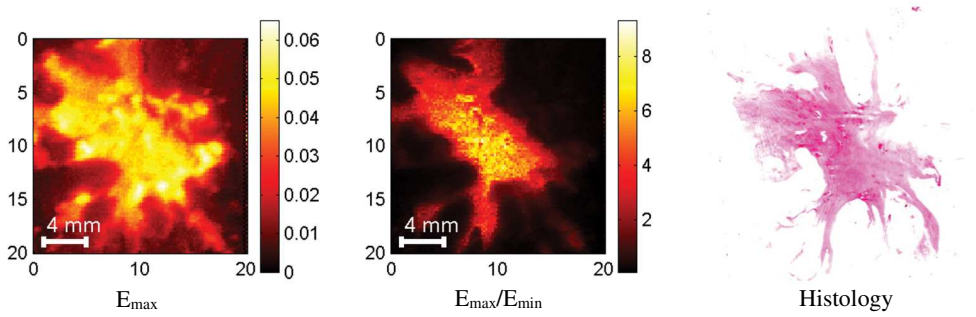

Fig. 1. This figure shows two terahertz images generated using the maximum of the reflected pulse (E_{max}) and the ratio between maximum and minimum of the reflected pulse (E_{max}/E_{min}). In the Emax image all the tissue is shown, tumor with surrounding adipose tissue. In E_{max}/E_{min} only the tumor is visible and correlated well with the tumor shown in the histology image.

Statistics show that 1 in 8 women will be diagnosed with breast cancer at some point during their lives [13]. With over 194,000 new cases of breast cancer being diagnosed annually and more than 40,600 expected deaths for the year 2009 in the USA alone, breast cancer is the second most common form of cancer among women and the third leading cause of death from cancer after lung and colon cancers [13]. About 60% of women diagnosed with breast cancer will undergo breast conserving surgery, which entails removal of the cancer with a margin of normal tissue, normally 3-5 mm thick, whilst preserving as much healthy breast as possible. Failure to remove the entire cancer with an adequate margin of normal tissue occurs in about 15-20% of cases [14], resulting in an increased risk of local recurrence unless a second operation is undertaken to remove additional tissue, thus ensuring that all the disease has been excised. This potentially causes further physical morbidity, poorer cosmesis, increased risk of wound infection and increased psychological morbidity to the patient, and increased cost to health systems.

Currently, the techniques available to define the margins of a cancer intra-operatively are clinical palpation, excised specimen mammography or cytological or frozen section assessment. These techniques all have inherent limitations; manual palpation is crude and will miss non-palpable lesions such as ductal carcinoma *in situ* (DCIS), specimen mammography will detect gross cancer or microcalcifications extending close to the margin but will miss lesions that are not visible on x-ray, and cytological evaluation or frozen section require the availability of an experienced cyto- or histopathologist and permits only focal assessment of the margin [15]. Post-operatively, the excised specimen undergoes histological examination including assessment of excision margins to determine whether the cancer has been fully removed. This process may take several days, and introduces delays in subsequent management.

With the increasing use of primary chemotherapy and endocrine therapy to downstage disease and with detection of smaller cancers through population-based breast screening programs, it is likely that the number of patients undergoing breast conserving surgery (as opposed to mastectomy) will continue to increase. There is clearly a need for a more accurate method of defining the margins of cancer excision intra-operatively, and THz imaging offers a promising solution.

In the study by Fitzgerald *et al.* [6] they were able to identify contrast between cancers and healthy tissue in the breast, however the origin of this contrast was somewhat unclear. This study aims to measure the optical characteristics of both healthy and diseased breast tissue in the THz region via time-domain THz pulsed spectroscopy (TPS) with the hope of better understanding the mechanisms that cause this contrast.

#110869 - $15.00 USD Received 4 May 2009; revised 29 Jun 2009; accepted 29 Jun 2009; published 7 Jul 2009

2. Materials and Methods

2.1 Samples

In this study, at least two specimens (typically 5-10 mm^3 in size) of breast cancer and healthy breast tissue from 20 non-consecutive female patients were obtained for this study over a period from April 2005 to May 2007. The tissue specimens were excess to histopathological diagnostic requirements and written informed consent was obtained from each patient for their tissue to be used for research purposes and approval for this study was granted by the local research ethics committee.

To ensure the moisture content of the specimens remained constant they were stored in a refrigerated, humidified environment. Samples for the THz spectroscopy measurement were prepared by cutting slices of tissue, with a uniform thickness of approximately 500 μm and 5 mm in diameter which were immediately placed into a specially designed holder, as used for measurements in a previous study of basal cell carcinoma [12]. Approximately two to three slices were cut from both the cancererous and the healthy tissue specimens, totaling 105 samples from all patients. The sample holder consisted of two quartz plates, or "windows", separated by a spacer of chosen thickness to match the thickness of the sliced sample being measured. Thus when the quartz plates were fastened together there was not excessive pressure on the tissue sample but also no air gaps between the sample and the quartz windows; this ensured the sample was held firmly and parallel between the plates. An aperture was chosen for smaller samples to ensure that the beam was only transmitted through the sample and that "edge effects" were not encountered. All samples were measured using the TPIspectra1000 (described below) within 24 hours of surgery and at room temperature.

Once measurement was complete the samples were placed in 10% buffered formalin, subsequently routinely processed and embedded in paraffin wax. Four micron thick sections were then taken and stained with hematoxylin and eosin (H&E). Multiple histology sections were taken from each tissue sample measured and were checked for consistency within the sample. If the content of the histology sections were too inconsistent we decided that the sample was too heterogeneous and thus not included in data averaging. Representative sections from the measured sample were then examined by a Consultant Breast Pathologist (SP or EP) who identified the percentage content of "fat" (healthy adipose tissue), "fibrous" (healthy fibrous breast tissue) and "cancer" in each section. Samples that contained more than 50% of any one tissue type were classified by their predominant component into one of the corresponding groups, namely "healthy fat", "healthy fibrous" and "cancer". Only completely "healthy" samples (i.e. 0% cancer content) were placed in either of the healthy groups (fat or fibrous). Of the 105 tissue samples from the specimens 74 could be grouped in this way.

2.2 THz Spectrometer

Time-domain terahertz pulsed spectroscopy measurements were taken using a TPI 1000© system, see Fig. 2 for a schematic. The system uses a Ti:Sapphire laser to produce 90 fs 800 nm pulses at a rate of 80 MHz that are incident on a photoconductive emitter (gold electrodes in a "bow tie" arrangement on a GaAs substrate) to produce electron-hole pairs that are then accelerated by an electric field placed across the electrodes. The relaxation of the charge carriers radiates THz pulses of bandwidth 0.1 – 4.0 THz. The THz pulses are transmitted through the sample and are incident on a photoconductive detector (similar to the emitter) that also has incident 90fs 800nm pulses derived from splitting the beam of the previously mentioned laser after being passed through a delay line, the length of which is periodically varied to produce a time gated detection mechanism that samples the THz pulses with a very high signal to noise ratio (10,000:1 at 1 THz). With the tissue sample in place the signal to noise ratio depends on the absorption coefficient and the thickness of the sample; typically it was about 500:1. The space through which the THz beam passes is purged with nitrogen gas to reduce absorption caused by water vapor in the air. The system is described in more detail by Taday and Newnham [16].

#110869 - $15.00 USD Received 4 May 2009; revised 29 Jun 2009; accepted 29 Jun 2009; published 7 Jul 2009

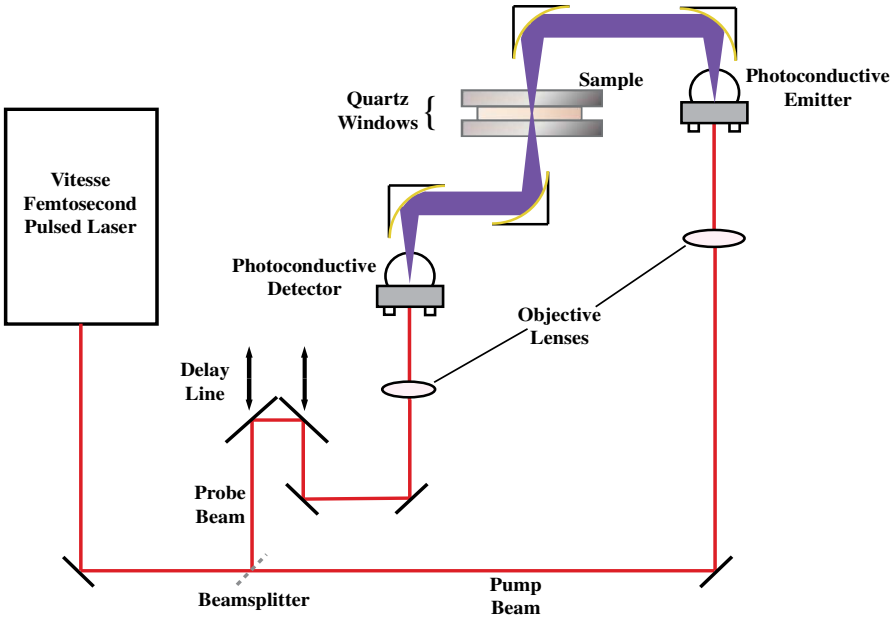

Fig. 2. Schematic representation of a TPI spectra1000©

2.3 Theory

To calculate the refractive index and absorption coefficient of a sample, measurement of a "reference" pulse (transmitted through the windows in the absence of a sample or spacer but with an aperture in place appropriate to the sample intended for measurement), as well a "sample pulse" (that is transmitted through the windows, sample and appropriate aperture) are required (see Fig. 3). A Fast Fourier Transform (FFT) is performed on the detected pulses to obtain the electric field in the frequency domain. The frequency dependent sample and reference electric fields are given by $E_S(w)$ and $E_R(w)$ respectively. The ratio of these can be written as a complex number with magnitude A and phase $\Delta\varphi$ as in Eq. (1):

$$\frac{E_S}{E_R} = Ae^{i\Delta\varphi}. \tag{1}$$

Thus $\Delta\varphi$ is the phase change of the measured pulses transmitted through a sample. The frequency dependent refractive index of the sample, n, is then given by:

$$n = 1 + \frac{c}{\omega \cdot d}\Delta\varphi; \tag{2}$$

where d is the sample thickness and c is the speed of light. The absorption coefficient (α) of the sample is given by:

$$\alpha = -\frac{2}{d}\ln\left\{\frac{\left(n+n_Q\right)^2}{4nn_Q}\cdot A\right\}. \tag{3}$$

The first part of the logarithmic term in Eq. (3) for the absorption coefficient corrects for losses due to Fresnel reflections at the interfaces between the sample and the quartz windows, where n_Q is the refractive index of quartz. The refractive index and absorption coefficient spectra for each of the samples were calculated and the average of these was taken for each

#110869 - $15.00 USD Received 4 May 2009; revised 29 Jun 2009; accepted 29 Jun 2009; published 7 Jul 2009

group of tissue types. Most of the tissue samples were not homogeneous and contained a mixture of tissue types. To extract the properties of the constituent tissue types the refractive indices and absorption coefficients were averaged linearly by assuming that any reflections and scattering caused by heterogeneities within samples were negligible. In this way, the refractive index and absorption coefficient for samples of pure fat, fibrous and cancer tissue were found by solving for each tissue type using a linear equation describing the contribution of each tissue type to the averaged refractive index and absorption coefficients of each group.

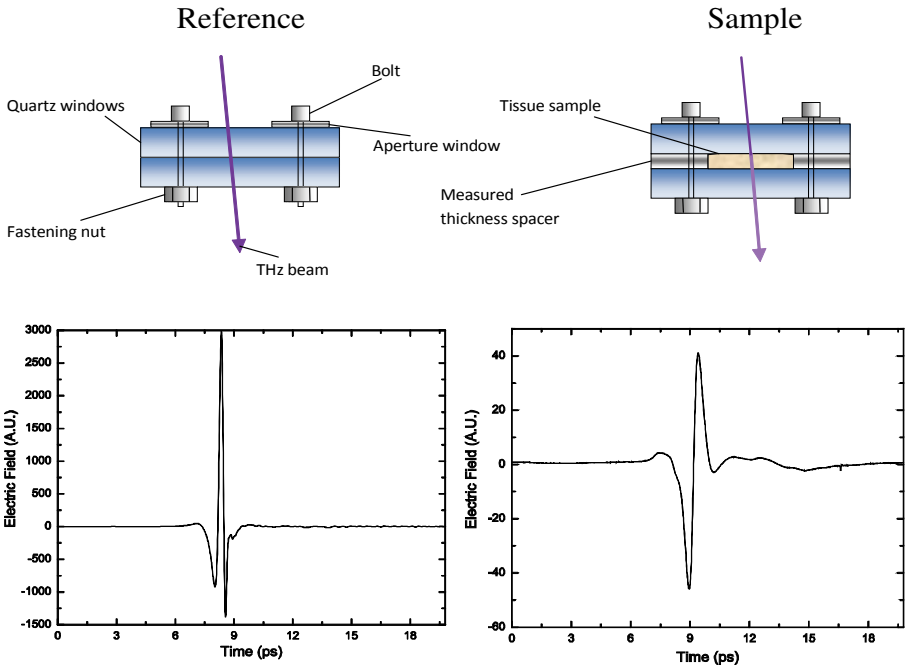

Fig. 3. Schematic representation of a sample holder set up for measuring reference and sample pulses and typical respective pulses.

Consider the transmission of THz radiation through multiple joined media that are not mixed at a molecular level. We can calculate the refractive index we expect to measure based on the thickness contribution of each type of media and their respective refractive indices. Equations (4)–(9) show us the refractive indices can be simply averaged in this scenario. Equation (2) can be rearranged to give the phase change as a function of the refractive index:

$$\Delta\varphi = \frac{(n-1)\cdot d\cdot\omega}{c}. \tag{4}$$

As the pulse propagates from medium 1 to 2 (denoted by the subscripts 1 and 2) the phase changes can be combined linearly giving the following result:

$$\Delta\varphi_{1,2} = \Delta\varphi_1 + \Delta\varphi_2. \tag{5}$$

For a two part system d_1/d and d_2/d are the percentage content of the two media by spatial occupation, given by:

$$\Delta\varphi_{1,2} = \frac{(n_1-1)\cdot d_1\cdot\omega}{c} + \frac{(n_2-1)\cdot d_2\cdot\omega}{c} \tag{6}$$

and

#110869 - $15.00 USD Received 4 May 2009; revised 29 Jun 2009; accepted 29 Jun 2009; published 7 Jul 2009

$$\Delta\varphi_{1,2} = \frac{d \cdot \omega}{c} \cdot ((n_1 - 1)\frac{d_1}{d} + (n_2 - 1)\frac{d_2}{d}. \quad (7)$$

Equation (7) is then substituted into Eq. (2) to obtain the refractive index:

$$n = 1 + ((n_1 - 1)\frac{d_1}{d} + (n_2 - 1)\frac{d_2}{d}). \quad (8)$$

For a two part system, $d = d_1 + d_2$, and so $1\text{-}d_1/d\text{-}\ d_2/d = 0$ and Eq. (8) can be simplified to obtain Eq. (9):

$$n = n_1\frac{d_1}{d} + n_2\frac{d_2}{d}. \quad (9)$$

In general for an l part system:

$$n_{Measured} = n_1\frac{d_1}{d} + n_2\frac{d_2}{d} + \ldots + n_l\frac{d_l}{d}. \quad (10)$$

Similarly this can be applied to the equations for absorption coefficient in Eq. (2) giving Eq. (11).

$$\alpha_{Measured} = \alpha_1\frac{d_1}{d} + \alpha_2\frac{d_2}{d} + \ldots + \alpha_l\frac{d_l}{d}. \quad (11)$$

Equations (10) and (11) were used to calculate the average measured values of refractive index and absorption coefficient for each tissue group and the fractional contributions each of the tissue types made to these groups. These equations were then solved simultaneously to predict the refractive index and absorption coefficient we would expect if we were to measure "pure" samples of each tissue type.

These spectra were used to simulate the impulse responses of each tissue type expected to be seen if imaging the tissue (in a pure, homogeneous form) in reflection. This was done by taking the inverse FFT (iFFT) of the ratio between the reflectivity at the interface between quartz and tissue as shown in Eq. (15) and the reflectivity of the quartz-air interface present when taking a reference for imaging. The frequency (ω) dependent reflectivity of the sample $r_s(\omega)$ is given by:

$$r_S(\omega) = \frac{\left(\hat{n}_Q(\omega) - \hat{n}_S(\omega)\right)}{\left(\hat{n}_Q(\omega) + \hat{n}_S(\omega)\right)}, \quad (12)$$

and for the reference is given by:

$$r_R(\omega) = \frac{\left(\hat{n}_Q(\omega) - \hat{n}_0(\omega)\right)}{\left(\hat{n}_Q(\omega) + \hat{n}_0(\omega)\right)}. \quad (13)$$

Where $\hat{n}_Q$ and $\hat{n}_0$ are the frequency dependent complex refractive indices of the quartz windows and air, respectively. For clarity, $\hat{n}$ in general is given by:

$$\hat{n}(\omega) = n(\omega) - i\frac{c}{2\omega}\alpha(\omega) \quad (14)$$

The impulse response is calculated using:

#110869 - $15.00 USD Received 4 May 2009; revised 29 Jun 2009; accepted 29 Jun 2009; published 7 Jul 2009

$$impulse(t) = iFFT\left[FFT(filter).\frac{r_S(\omega)}{r_R(\omega)} \right], \quad (15)$$

and "*filter*" is a double Gaussian filter chosen to remove high and low frequency noise [17].

3. Results and Discussion

Out of the 105 breast tissue samples measured 74 were found to be sufficiently homogeneous and successfully classified: 33 as cancer, 22 as healthy fibrous and 19 as healthy fat. Table 1 shows the average content of these three groups. As the maximum length scale of heterogeneities within the regions of the individual specimens was about 500 μm and the THz beam spot size was about 1mm in diameter, our assumption that the heterogeneities within specimens will appear as a homogeneous mix of the various tissue types is valid to a first approximation. The group averages of the spectra from these specimens were used to calculate the absorption and refractive index spectra shown in Fig. 4 using the methods described above. The error bars displayed represent 95% confidence intervals derived from the standard error of the mean. The error bars for the refractive index are constant for fibrous tissue and fat but are slightly larger at high and low frequencies in the for the cancer samples, this is due to low signal in these ranges caused by attenuation through the sample leading to errors in "unwrapping" the phase.

Table 1. List of the average percentage of each tissue classification in groups.

Group / Tissue Type	Healthy Fat	Healthy Fibrous	Cancer
Fat (%)	89.7	19.1	3.1
Fibrous (%)	10.3	80.9	5.8
Cancer (%)	0	0	91.1

There is a clear difference in the refractive indices between all tissue types and also a difference between the absorption coefficient of fat and the other two tissue types. However the difference in absorption between fibrous tissue and cancer is not so clear and for most of the range the error bars overlap. For the absorption graph (Fig. 4, left) the shape of the curve of the cancer is very similar to fibrous tissue. However, the transmitted signal is lower due to the increased attenuation in the cancer. The attenuation is a combination of absorption and scattering and it would be impossible with this type of measurement to determine the contribution from each mechanism. If one looks at studies on dehydrated, wax embedded tissue samples, attenuation also increases for regions of cancer, which can only result from structural changes which, in turn, changes the scattering properties [18,19]. However, in freshly excised tissues samples, which closely match *in vivo* conditions, their water content will be in the region of 80%. Thus the large absorption due to the high water content leads to the assumption that absorption is the dominant attenuation mechnism and scattering negligible in comparison.

#110869 - $15.00 USD Received 4 May 2009; revised 29 Jun 2009; accepted 29 Jun 2009; published 7 Jul 2009

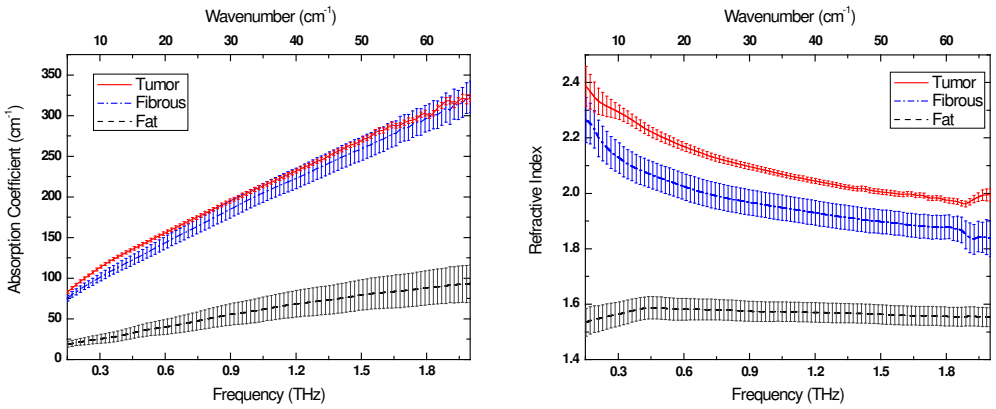

Fig. 4. Graphs showing the absorption coefficients and refractive indices of the three tissue types (tumor, fibrous and fat). Error bars represent 95% confidence intervals.

Figure 5 shows the difference between the absorption coefficient and refractive index spectra of fibrous and cancer samples more clearly. The maximum difference of both spectra occurs at 0.32 THz. The increase in the difference at 0.32 THz cannot be solely attributed to an increase in tetrahedral (free) water as there is no distinct feature at 0.32 THz in free water so this is likely to be caused by association of water with a functional group such as proteins, or even caused by increased protein density alone [20]. The increase in refractive index over the spectral range is likely to be caused by an increase in free water because it has a higher refractive index than that of tissue. A similar increase in the absorption spectrum is not seen because the absorption spectrum is already very close to that of water [11]. For completeness, the dielectric constants have also been calculated and are shown in Fig. 6.

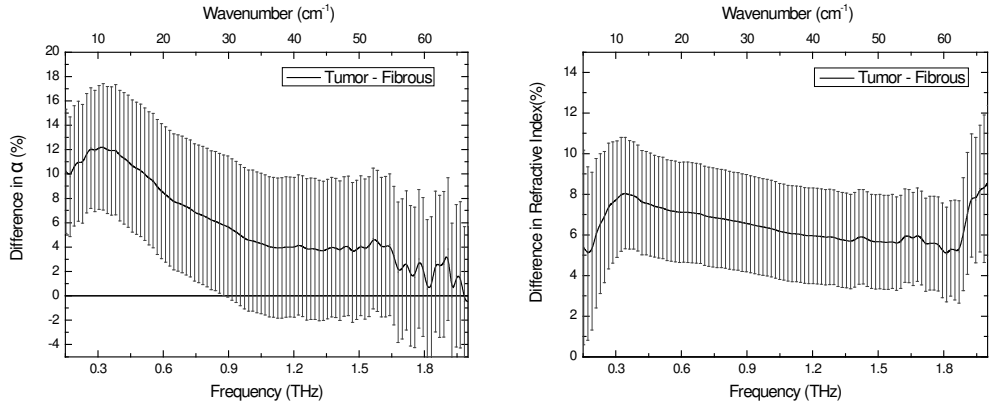

Fig. 5. Graphs showing the difference in absorption (α) and refractive index (n) spectra between tumor and healthy fibrous tissue as a percentage of the healthy fibrous spectra.

#110869 - $15.00 USD Received 4 May 2009; revised 29 Jun 2009; accepted 29 Jun 2009; published 7 Jul 2009

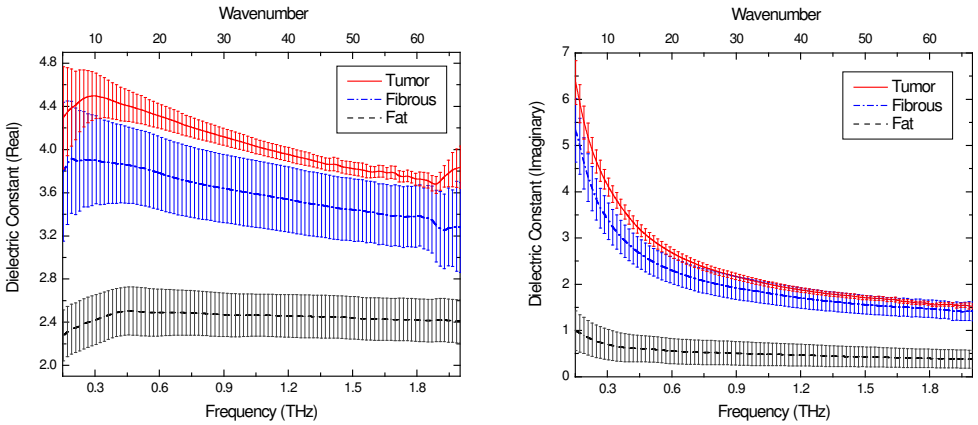

Fig. 6. Graphs showing the real and imaginary parts of the dielectric constants. Error bars represent 95% confidence intervals.

Using these spectral data, impulse functions were simulated from a Fresnel-based model [7] of homogeneous "pure" samples of each breast tissue type when imaging in reflection, shown in Fig. 7. There is an obvious difference between the impulse function of fat and that of cancer and fibrous tissue. The differences between the impulse functions of cancer and fibrous tissue are more subtle; the clearest difference is that of the peak height. These simulated impulse functions are consistent with those reported from the TPI reflection imaging study by Fitzgerald *et al* [6] and suggest that the differences in the optical properties of the tissues are large enough to be detected in reflection geometry.

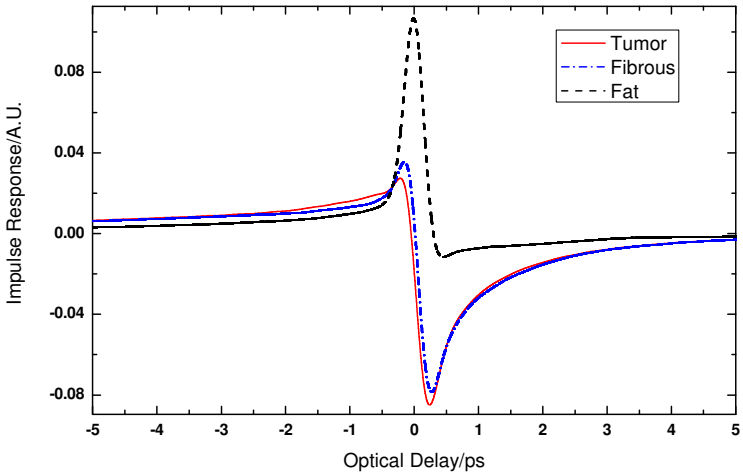

Fig. 7. Simulated impulse functions

4. Conclusions

In this study we successfully measured the refractive index and absorption coefficient spectra of healthy and diseased breast tissue from 20 breast cancer patients. Comparisons of the differences between the spectra of different tissue types were made. It is seen that breast cancer has a higher refractive index than both healthy fatty and healthy fibrous tissue with the greatest difference being at 0.32 THz as well as having a slight increase of absorption around 0.32 THz compared with fibrous breast tissue. Simulations were carried out to predict the impulse responses from performing THz pulsed reflection imaging on these tissues. A large difference was seen, as expected, between the impulse response of healthy fat and those of healthy fibrous and breast cancer tissues. A difference in peak height of about 60% was seen

#110869 - $15.00 USD Received 4 May 2009; revised 29 Jun 2009; accepted 29 Jun 2009; published 7 Jul 2009

on the impulse responses between cancer and healthy fibrous tissue. Such difference encourages the development of medical devices based on THz technology. Insomuch, an intra-operative surgical tool has been developed, which detects differences in THz signals reflected from diseased and healthy breast tissue [21]. Such technologies will add to the arsenal of techniques available to clinicians for improvement of cancer treatment and healthcare in general.

In conclusion, the contrast seen when imaging breast cancer in reflection is mainly caused by an increase in the refractive index between cancer and healthy tissues and also in part due to an increase in the absorption coefficient. The root cause of the increases in these fundamental properties is yet to be determined.

Acknowledgment

Part of this study was funded by the UK Department of Heath, Health Technology Devices Program (HTD158).

#110869 - $15.00 USD Received 4 May 2009; revised 29 Jun 2009; accepted 29 Jun 2009; published 7 Jul 2009